Synthesis, crystal structures, electrochemical and protein-binding properties of ferrocene–indole conjugates

Kenneth Kam-Wing Lo,*[a] Jason Shing-Yip Lau[a] and Nianyong Zhu[b]

Received (in Montpellier, France) 26th June 2006, Accepted 3rd August 2006
First published as an Advance Article on the web 24th August 2006
DOI: 10.1039/b609052d

This paper describes the synthesis, characterisation and electrochemical properties of three redox-active ferrocene–indole compounds, *N*-(ferrocenylmethylenyl)tryptamine (Fc–CH=NC_2H_4-indole) (Fc1), *N*-(ferrocenylmethyl)tryptamine (Fc–$CH_2NHC_2H_4$-indole) (Fc2) and indole-3-(*N*-(6-(*N*-ferrocenylmethyl)aminohexyl))carboxamide (Fc–$CH_2NHC_6H_{12}$NHCO-indole) (Fc3). The X-ray crystal structures of Fc1 and Fc2 have been investigated. The recognition of the redox-active ferrocene–indole compounds Fc2 and Fc3 by indole-binding proteins including bovine serum albumin and tryptophanase has been studied by electrochemical and luminescence titrations and enzyme inhibition assays.

Introduction

Indole and its derivatives such as indole-3-acetic acid, serotonin and melatonin play important roles in plant, animal and human physiology.[1–6] The recognition of these compounds by indole-binding proteins has been given much attention. To study the substrate-binding properties of these receptors, various approaches such as radioactive and fluorescent labels,[7–11] enzyme inhibition assays[12] and biotinylated indole compounds[13] have been utilised. Recently, we have incorporated an indole unit into various luminescent transition metal complexes such as rhenium(I) and ruthenium(II) polypyridines to afford probes for indole-binding proteins.[14] To the best of our knowledge, electrochemical probes for these biological receptors have not been explored. We anticipate that redox-active ferrocene can be employed as a new type of electrochemical reporter for this important class of proteins.

In this paper, we report the synthesis, characterisation and electrochemical properties of three redox-active ferrocene–indole compounds, *N*-(ferrocenylmethylenyl)tryptamine (Fc–CH=NC_2H_4-indole) (Fc1), *N*-(ferrocenylmethyl)tryptamine (Fc–$CH_2NHC_2H_4$-indole) (Fc2) and indole-3-(*N*-(6-(*N*-ferrocenylmethyl)aminohexyl))carboxamide (Fc–$CH_2NHC_6H_{12}$NHCO-indole) (Fc3) (Scheme 1). The X-ray crystal structures of Fc1 and Fc2 have been investigated. The recognition of the ferrocene–indole compounds Fc2 and Fc3 by indole-binding proteins including bovine serum albumin (BSA) and tryptophanase (TPase) has been studied by electrochemical and luminescence titrations and enzyme inhibition assays.

Experimental

Materials and reagents

All solvents were of analytical grade and purified according to published procedures.[15] Ferrocenecarboxaldehyde (International Lab), tryptamine (Acros), $NaBH_4$ (Acros), indole-3-carboxylic acid (Acros), *tert*-butyl *N*-(6-aminohexyl)-carbamate hydrochloride (International Lab), triethylamine (Acros), *N*-hydroxysuccinimide (NHS) (Acros), *N*,*N*′-dicyclohexylcarbodiimide (DCC) (Acros), trifluoroacetic acid (TFA) (International Lab), L-serine (Acros), pyridoxal 5-phosphate (Sigma), lactate dehydrogenase (LDH) (Calbiochem), NADH (Calbiochem), BSA (Calbiochem) and TPase (Sigma) were used without purification. Tetra-*n*-butylammonium hexafluorophosphate (TBAP) (Aldrich) was recrystallised from hot ethanol and dried *in vacuo* at 110 °C before use. The luminescent label [Ir(ppy)$_2$(phen–N=C=S)](PF_6) (Hppy = 2-phenylpyridine, phen–N=C=S = 5-isothiocyanato-1,10-phenanthroline) was prepared according to reported procedures.[16]

Syntheses

Fc–CH=NC_2H_4-indole (Fc1). A mixture of ferrocenecarboxaldehyde (204 mg, 0.95 mmol) and tryptamine (153 mg, 0.95 mmol) in 25 mL of EtOH was refluxed under an inert atmosphere of nitrogen for 6 h. The orange mixture was then filtered and the filtrate was evaporated to dryness to give an orange solid. Subsequent recrystallisation of the product from a diethyl ether/petroleum ether (bp 40–60 °C) mixture afforded orange crystals. Yield = 248 mg (74%). ^{1}H NMR (300 MHz, acetone-d_6, 298 K, relative to TMS): δ 10.00 (s, br, 1H, NH of indole), 8.07 (s, 1H, Fc–C*H*), 7.64 (d, 1H, J = 7.6 Hz, H4 of indole), 7.35 (dd, 1H, J = 7.0 and 1.3 Hz, H7 of indole), 7.19 (d, 1H, J = 2.3 Hz, H2 of indole), 7.10–6.99 (m, 2H, H5 and H6 of indole), 4.59 (t, 2H, J = 1.8 Hz, H2 and H5 of ferrocene), 4.61 (t, 2H, J = 1.9 Hz, H3 and H4 of ferrocene), 4.03 (s, 5H, H1′–H5′ of ferrocene), 3.75 (dt, 2H, J = 7.0 and 1.3 Hz, NCH_2), 3.06 (t, 2H, J = 7.0 Hz, NCH_2CH_2). IR (KBr) ν/cm^{-1}: 3423 (m, N–H), 1642 (s, C=N). Positive-ion ESI-MS ion cluster at m/z 357 {M + H}$^+$. Anal. calc. for $C_{21}H_{20}N_2Fe$: C, 70.80; H, 5.66; N, 7.86. Found: C, 70.50; H, 5.72; N, 7.86%. UV/Vis [λ_{abs}/nm (ε/dm^3 mol^{-1} cm^{-1})]: CH_2Cl_2, 275 (11 180), 289 sh (7365), 322 (1255), 346 sh (835), 450 (385); MeOH, 275 (10 395), 289 sh (7545), 327 (1440), 358 sh (835), 452 (450).

[a] *Department of Biology and Chemistry, City University of Hong Kong, Tat Chee Avenue, Kowloon, Hong Kong, P. R. China. E-mail: bhkenlo@cityu.edu.hk; Fax: +852 2788 7406; Tel: +852 2788 7231*
[b] *Department of Chemistry, The University of Hong Kong, Pokfulam Road, Hong Kong, P. R. China*

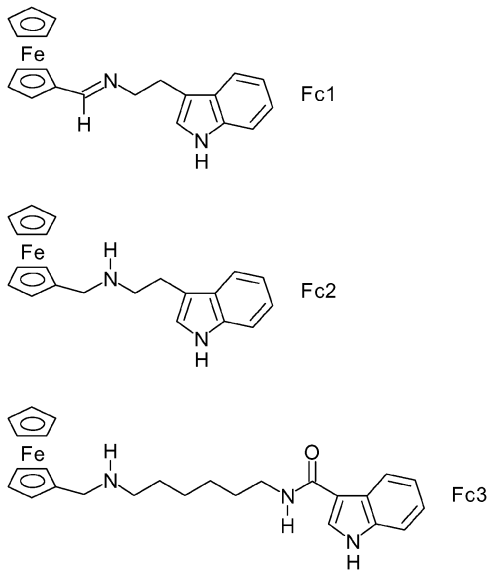

Scheme 1 Structures of Fc1, Fc2 and Fc3.

Fc–$CH_2NHC_2H_4$-indole (Fc2). A mixture of Fc1 (121 mg, 0.34 mmol) and $NaBH_4$ (26 mg, 0.68 mmol) in 20 mL of EtOH was stirred under an inert atmosphere of nitrogen for 12 h. The mixture was then evaporated to dryness to give an orange solid, which was then dissolved in CH_2Cl_2. The solution was filtered and the filtrate was evaporated to dryness to give an orange-yellow solid. Subsequent recrystallisation of the product from a diethyl ether/petroleum ether (bp 40–60 °C) mixture afforded orange-yellow crystals. Yield = 97 mg (80%). ^{1}H NMR (300 MHz, acetone-d_6, 298 K, relative to TMS): δ 10.06 (s, br, 1H, NH of indole), 7.64 (d, 1H, J = 7.6 Hz, H4 of indole), 7.36 (d, 1H, J = 8.2 Hz, H7 of indole), 7.21 (s, 1H, H2 of indole), 7.12–7.00 (m, 2H, H5 and H6 of indole), 4.14 (s, 2H, H2 and H5 of ferrocene), 4.02 (s, 2H, H3 and H4 of ferrocene), 3.92 (s, 5H, H1′–H5′ of ferrocene), 3.46 (s, 2H, Fc–CH_2), 2.97 (s, 4H, NHC$_2H_4$), 2.87 (s, br, 1H, NHC$_2$H$_4$). IR (KBr) ν/cm^{-1}: 3417 (m, N–H). Positive-ion ESI-MS ion cluster at m/z 359 $\{M + H\}^+$. Anal. calc. for $C_{21}H_{22}N_2Fe \cdot 0.25H_2O$: C, 69.53; H, 6.25; N, 7.72. Found: C, 69.63; H, 6.33; N, 7.67%. UV/Vis [λ_{abs}/nm (ε/dm^3 mol^{-1} cm^{-1})]: CH_2Cl_2, 272 (6840), 290 sh (4785), 325 (60), 439 (85); MeOH, 275 (6535), 287 sh (4865), 323 sh (90), 440 (100).

Indole-3-carboxylic acid succinimidyl ester. A mixture of indole-3-carboxylic acid (600 mg, 3.72 mmol), NHS (544 mg, 4.72 mmol) and DCC (845 mg, 4.10 mmol) in 30 mL of DMF was stirred under an inert atmosphere of nitrogen for 12 h. The mixture was then evaporated under vacuum to give a white solid. The solid was dissolved in CH_2Cl_2 and the solution was then filtered. The filtrate was evaporated to dryness to give a white solid, which was then recrystallised from a CH_2Cl_2/petroleum ether (bp 40–60 °C) mixture to afford the product as white crystals. Positive-ion ESI-MS ion cluster at m/z 258 $\{M\}^+$.

Fc–$CH_2NHC_6H_{12}$NHCO-indole (Fc3). A mixture of indole-3-carboxylic acid succinimidyl ester (809 mg, 3.14 mmol), *tert*-butyl *N*-(6-aminohexyl)carbamate hydrochloride (794 mg, 3.14 mmol) and 200 μL of triethylamine in 50 mL of DMF was stirred under an inert atmosphere of nitrogen for 12 h. The mixture was then evaporated under vacuum to give a yellow oil. It was dissolved in CH_2Cl_2 and the solution was then filtered. TFA (15 mL) was added to the filtrate and the solution was stirred at room temperature for 12 h. The mixture was then evaporated to dryness. To the solid was added a solution of ferrocenecarboxaldehyde (760 mg, 3.54 mmol) and 200 μL of triethylamine in 50 mL of EtOH. The solution was refluxed under an inert atmosphere of nitrogen for 4 h. It was cooled to room temperature and then $NaBH_4$ (536 mg, 14.16 mmol) was added. The mixture was stirred under an inert atmosphere of nitrogen for 12 h and then evaporated to dryness to give a brown solid. Subsequent recrystallisation of the product from a diethyl ether/petroleum ether (bp 40–60 °C) mixture afforded brown crystals. Yield = 1.13 g (70%). ^{1}H NMR (300 MHz, acetone-d_6, 298 K, relative to TMS): δ 10.08 (s, br, 1H, NH of indole), 8.14 (s, 1H, NHCO), 7.61 (d, 1H, J = 7.6 Hz, H4 of indole), 7.39 (d, 1H, J = 7.9 Hz, H7 of indole), 7.19 (s, 1H, H2 of indole), 7.15–7.00 (m, 2H, H5 and H6 of indole), 4.30 (s, 2H, Fc–CH_2), 4.24 (d, 2H, J = 1.8 Hz, H2 and H5 of ferrocene), 4.15 (d, 5H, J = 1.2 Hz, H1′–H5′ of ferrocene), 4.09 (d, 2H, J = 1.8 Hz, H3 and H4 of ferrocene), 3.36 (t, 2H, J = 4.4 Hz, CH_2NHCO), 2.42 (t, 2H, J = 5.1 Hz, Fc–CH_2NHCH_2), 1.63–1.42 (m, 8H, NHCH$_2$C$_4H_8$CH$_2$NHCO). IR (KBr) ν/cm^{-1}: 3417 (m, N–H). Positive-ion ESI-MS ion cluster at m/z 457 $\{M\}^+$. Anal. calc. for $C_{26}H_{31}N_3OFe \cdot 2H_2O$: C, 63.29; H, 7.15; N, 8.52. Found: C, 63.40; H, 7.39; N, 8.73%. UV/Vis [λ_{abs}/nm (ε/dm^3 mol^{-1} cm^{-1})]: CH_2Cl_2, 271 (9505), 285 sh (7645), 316 sh (730), 430 sh (265); MeOH, 279 (8675), 285 sh (7940), 318 sh (440), 430 sh (180).

Instrumentation and methods

^{1}H NMR spectra were recorded on a Varian Mercury 300 MHz NMR spectrometer at 298 K. Positive-ion ESI mass spectra were recorded on a Perkin Elmer Sciex API 365 mass spectrometer. IR spectra were recorded on a Perkin Elmer 1600 series FT-IR spectrophotometer. Elemental analysis was carried out on an Elementar Analysensysteme GmbH Vario EL elemental analyser. Electronic absorption spectra were recorded on a Hewlett-Packard 8453 diode array spectrophotometer. Steady-state emission spectra were recorded on a Spex Fluorolog-2 Model F 111 or a Fluoromax-3 fluorescence spectrophotometer. Electrochemical experiments were performed on a CH Instruments Electrochemical Workstation CHI750A at 298 K with a two-compartment glass cell with a working volume of 500 μl. A platinum gauze counter electrode was accommodated in the working electrode compartment. The working electrode was a glassy carbon electrode. The reference electrodes were Ag/$AgNO_3$ (0.1 M in CH_3CN) and Ag/AgCl (3 M aqueous KCl) electrodes for measurements in CH_3CN and aqueous buffer solutions, respectively. The reference electrode compartment was connected to the working electrode compartment *via* a Luggin capillary. Solutions for electrochemical measurements were degassed with pre-purified argon gas. All potentials were referred to SCE.

Unsubstituted ferrocene was used as an internal reference for non-aqueous solution measurements. Under our experimental conditions, the reversible ferrocenium/ferrocene couple occurred at +0.11 V *vs.* $Ag/AgNO_3$ in CH_3CN at 298 K.

Crystal structure determination

Single crystals of Fc1 and Fc2 that were suitable for X-ray crystallographic studies were obtained by layering petroleum ether (bp 40–60 °C) over concentrated CH_2Cl_2 solutions of the compounds. Crystals of Fc1 and Fc2 of dimensions 0.6 × 0.2 × 0.1 and 0.5 × 0.3 × 0.15 mm, respectively, were mounted in glass capillaries and used for data collection at −20 °C on a MAR diffractometer with a 300-mm image plate detector using graphite monochromatised Mo-Kα radiation. Data collections for Fc1 and Fc2 were made with 2° and 3° oscillation steps of ϕ, respectively, 10 min exposure time and scanner distance at 120 mm. A total of 75 images were collected for Fc1 and 60 images were collected for Fc2. The images were interpreted and intensities integrated using the programme DENZO.[17] The structures were solved by direct methods employing the programme SIR-97.[18] Iron and most non-hydrogen atoms were located according to direct methods and successive least-square Fourier cycles. The positions of other non-hydrogen atoms were found after successful refinement by full-matrix least-squares using the programme SHELXL-97.[19] One crystallographic asymmetric unit of Fc1 or Fc2 consists of one formula unit. In the final stage of least-squares refinement, all non-hydrogen atoms were refined anisotropically. Hydrogen atoms were generated by the programme SHELXL-97.[19] The positions of the hydrogen atoms were calculated based on a riding mode with thermal parameters equal to 1.2 times that of the associated carbon atoms, and participated in the calculation of final *R*-indices.

Crystal data and a summary of data collection and refinement details for Fc1 and Fc2 are given in Table 1.

CCDC reference numbers 616828 and 616829. For crystallographic data in CIF or other electronic format see DOI: 10.1039/b609052d

Electrochemical titrations

The ferrocene–indole compound Fc2 or Fc3 (0.28 μmol) in 1 mL of 50 mM potassium phosphate buffer at pH 7.4/DMSO solution (9 : 1 v/v) was titrated with BSA (1.67 mM) in phosphate buffer. The peak current of the ferrocenium/ferrocene couple was measured by cyclic voltammetry after each addition. The binding constant (K_s) for the equilibrium between the probe Fc (Fc2 or Fc3), BSA and their adduct Fc–BSA,

$$\mathrm{Fc} + \mathrm{BSA} \overset{K_s}{\rightleftharpoons} \mathrm{Fc{-}BSA}$$

was obtained by fitting the experimental data to eqn (1) and (2):[20]

$$\frac{(i_o - i)}{(i_o - i_f)} = \frac{\left(b - \sqrt{b^2 - \frac{2K_s^2 C_t[\mathrm{BSA}]}{s}}\right)}{2K_s C_t} \qquad (1)$$

Table 1 Crystal data and summary of data collection and refinement for Fc1 and Fc2

	Fc1	Fc2
Empirical formula	$C_{21}H_{20}FeN_2$	$C_{21}H_{22}FeN_2$
M	356.24	358.26
Crystal size/mm	0.6 × 0.2 × 0.1	0.5 × 0.3 × 0.15
T/K	253	253
λ/Å	0.71069	0.71073
Crystal system	Orthorhombic	Monoclinic
Space group	$P2_12_12_1$	$P2_1/n$
a/Å	7.232(1)	6.907(1)
b/Å	9.890(2)	13.826(3)
c/Å	24.259(5)	17.936(4)
α/°	90	90
β/°	90	91.36(3)
γ/°	90	90
V/Å^3	1735.1(6)	1712.3(6)
Z	4	4
D_c/g cm^{-3}	1.364	1.390
μ(Mo-Kα)/mm^{-1}	0.872	0.884
F(000)	744	752
$2\theta_{max}$/°	50.70	50.88
Index ranges, hkl	−7 to 7, −11 to 11, −29 to 29	−7 to 7, −14 to 16, −21 to 21
Reflections collected	7098	9717
Independent reflections	2730	2946
No. of data for structural analysis	2394	2725
R_{int}[a]	0.0356	0.0318
R_1, wR_2 ($I > 2\sigma(I)$)[b]	0.0261, 0.0534	0.0284, 0.0850
GOF on F^2 [c]	0.875	1.046
Largest diff. peak, hole/e Å^{-3}	0.157, −0.203	0.245, −0.226

[a] $R_{int} = \sum|F_o^2 - F_o^2\,(\mathrm{mean})|/\sum[F_o^2]$. [b] $R_1 = \sum\|F_o| - |F_c\|/\sum F_o|$, $wR_2 = \{\sum[w(F_o^2 - F_c^2)^2]/\sum[w(F_o^2)^2]\}^{1/2}$. [c] GOF $= \{\sum[w(F_o^2 - F_c^2)^2]/(n-p)\}^{1/2}$, where n is the number of reflections and p is the total number of parameters refined. The weighting scheme is $w = 1/[\sigma^2(F_o^2) + (aP)^2 + (bP)]$, where P is $[2F_c^2 + \max(F_o^2,0)]/3$, $a = b = 0.0$ for Fc1; and $a = 0.0487$, $b = 0.0$ for Fc2.

$$b = 1 + K_s C_t + \frac{K_s[\mathrm{BSA}]}{2s} \qquad (2)$$

where: i_o = initial peak current, i = peak current measured at a BSA concentration [BSA], i_f = peak current of the fully bound species, C_t = total concentration of the probe Fc, s = binding-site size.

Conjugation of BSA with $[Ir(ppy)_2(phen\text{-}N{=}C{=}S)](PF_6)$[16]

The complex $[Ir(ppy)_2(phen–N{=}C{=}S)](PF_6)$ (4.2 mg, 4.76 μmol) dissolved in 100 μL of anhydrous DMSO was added to BSA (30.0 mg, 0.45 μmol) in 2 mL of 50 mM potassium phosphate buffer pH 7.4. The mixture was stirred gently at room temperature for 12 h. The solid residue was removed by centrifugation. The product Ir-BSA was purified with a PD-10 size-exclusion column and washed with phosphate buffer using a YM-30 microcon. Finally, the solution was concentrated to a volume of 500 μL and stored at 4 °C before use. The iridium-to-protein ratio of the labelled conjugate was determined to be *ca.* 2.8 by spectroscopic measurements.[21]

Luminescence titrations

The conjugate Ir-BSA (7.60 μM) in 2 mL of 50 mM potassium phosphate buffer pH 7.4 was titrated with the ferrocene–indole

compound Fc2 or Fc3 (6.30 mM) in DMSO. The emission intensity of the solution was measured after each addition. The binding constant (K_s) for the 1 : 1 complexation that controls the equilibrium between the probe Fc (Fc2 or Fc3), the luminescent conjugate Ir-BSA and their adduct Fc–(Ir-BSA),

$$\text{Fc} + \text{Ir-BSA} \overset{K_s}{\rightleftharpoons} \text{Fc}-(\text{Ir-BSA})$$

was obtained by a nonlinear least-squares fit of the emission intensity (X_s) *vs.* the concentration of the substrate (C_s) in the mixture according to eqn (3):[22]

$$X_s = X_o + \left(\frac{X_{lim} - X_o}{2C_o}\right) \left[C_o + C_s + \frac{1}{K_s} - \sqrt{\left(C_o + C_s + \frac{1}{K_s}\right)^2 - 4C_oC_s}\right] \quad (3)$$

where: C_o = initial concentration of the conjugate, X_o = emission intensity of the conjugate in the free state, X_{lim} = emission intensity of the conjugate in the probe-bound state.

Tryptophanase inhibition assays

The ferrocene–indole compound Fc2 or Fc3, ferrocene or free indole (0.10 μmol) in 100 μL of MeOH/phosphate buffer solution (2 : 1 v/v) was added to a mixture of pyridoxal 5-phosphate (0.125 μmol), LDH (8.225 U), NADH (0.70 μmol) and L-serine at various concentrations in 1.57 mL of 0.15 M potassium phosphate buffer pH 8.1 in an absorption cuvette. The temperature of the solution was thermostated at 37 °C for 5 min. The conversion of L-serine to pyruvate was initiated by adding tryptophanase (5 U in 830 μL of phosphate buffer) to the mixture. The concentration of L-serine in the cuvette varied from 100 to 800 mM. The percentage of inhibition of tryptophanase was determined by comparing the decrease of absorbance of the solution at 340 nm to that of the control. The Michaelis constants (K_m) for the enzyme activity were determined from plots of the linear transformation of the Michaelis–Menten equation, the Lineweaver–Burk transformation (eqn (4)):[23]

$$\frac{1}{v} = \frac{1}{V_{max}} + \frac{K_m}{V_{max}[S]} \quad (4)$$

where: v = reaction velocity, V_{max} = maximum reaction velocity, [S] = concentration of L-serine.

Results and discussion

Synthesis

Reaction of ferrocenecarboxaldehyde and tryptamine in refluxing alcohol under an inert atmosphere of nitrogen afforded Fc1. Since the imine group of Fc1 is susceptible to hydrolysis in aqueous solutions, we have also synthesised the reduced product (Fc2) that contains a secondary amine. To investigate the effects of distance between the redox-active ferrocene and the indole on the protein-binding properties, a spacer-arm has been employed in the design of Fc3. All the compounds Fc1–Fc3 were characterised by ^{1}H NMR spectrometry, positive-ion ESI-MS, IR spectroscopy and gave satisfactory microanalysis. The molecular structures of Fc1 and Fc2 have been studied by X-ray crystallography.

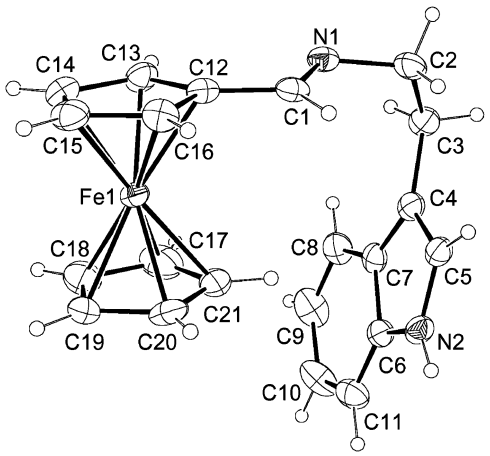

Fig. 1 Perspective drawing of Fc1 with the atomic numbering scheme. Thermal ellipsoids are shown at the 30% probability level.

Crystal structure determination

The perspective drawings of Fc1 and Fc2 are shown in Fig. 1 and 2, respectively. Selected bond distances and angles are listed in Tables 2 and 3, respectively. The two cyclopentadienyl rings of each compound are essentially co-planar, with dihedral angles of *ca.* 1.08° for Fc1 and 1.40° for Fc2. The Fe–C bond lengths ranged from 2.017(3) to 2.053(2) Å and are similar to those of related ferrocene derivatives.[24] The bond distance C(1)–N(1) of Fc1 (Fig. 1) was *ca.* 1.270(3) Å while C(11)–N(1) of Fc2 (Fig. 2) was *ca.* 1.468(3) Å, consistent with the double-bond nature of the former. The dihedral angles between the modified cyclopentadienyl ring and the indole moiety were *ca.* 73.11° for Fc1 and *ca.* 65.81° for Fc2.

Electrochemical properties

The electrochemical properties of the ferrocene–indole compounds have been studied by cyclic voltammetry. The electrochemical data of Fc1–Fc3 are listed in Table 4. The cyclic voltammograms of Fc1 and Fc2 in CH_3CN (0.1 M TBAP) at 298 K are shown in Fig. 3 and 4 as examples. At a sweep rate

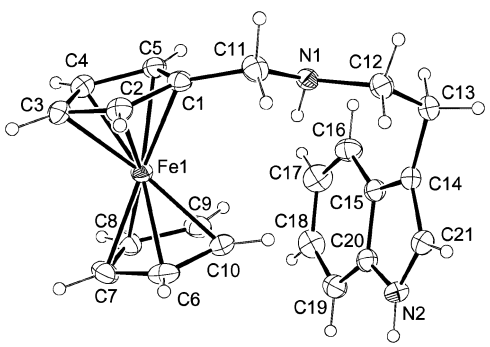

Fig. 2 Perspective drawing of Fc2 with the atomic numbering scheme. Thermal ellipsoids are shown at the 30% probability level.

Table 2 Selected bond distances (Å) and bond angles (°) for Fc1

C(1)–C(12)	1.456(3)	C(1)–N(1)	1.270(3)
C(2)–C(3)	1.517(3)	C(2)–N(1)	1.465(3)
C(3)–C(4)	1.509(3)	Fe(1)–C(12)	2.025(2)
Fe(1)–C(13)	2.030(2)	Fe(1)–C(14)	2.023(2)
Fe(1)–C(15)	2.039(2)	Fe(1)–C(16)	2.017(3)
Fe(1)–C(17)	2.032(3)	Fe(1)–C(18)	2.039(3)
Fe(1)–C(19)	2.038(2)	Fe(1)–C(20)	2.019(2)
Fe(1)–C(21)	2.038(3)		
C(1)–C(12)–C(13)	127.6(2)	C(1)–C(12)–C(16)	124.7(2)
C(1)–N(1)–C(2)	117.7(2)	C(2)–C(3)–C(4)	114.7(2)
C(3)–C(2)–N(1)	110.0(2)	C(3)–C(4)–C(5)	127.1(2)
C(3)–C(4)–C(7)	127.0(2)	C(12)–C(1)–N(1)	123.4(2)

of 100 mV s^{-1}, within a potential window of 0 and +0.8 V *vs.* SCE, Fc1 showed a reversible couple at *ca.* +0.49 (Fig. 3a) while Fc2 and Fc3 displayed similar couples at *ca.* +0.36 V *vs.* SCE (Table 4), which are assigned to ferrocenium/ferrocene couples.[24,25] The occurrence of this couple at a more positive potential for Fc1 than Fc2 and Fc3 is a consequence of the electron-withdrawing imine group of Fc1 and the electron-donating secondary amine groups of Fc2 and Fc3. Upon scanning to higher potentials, Fc1 showed additional quasi-reversible couples at *ca.* +0.96 and +1.27 V, which are attributable to the oxidation of the indole moiety (Fig. 3b).[14] This assignment is supported by the findings that unmodified indole displays similar features under the same experimental conditions. The indole oxidation significantly reduced the reversibility of the ferrocenium/ferrocene couple (Fig. 3b), suggestive of fouling of the electrode by the oxidised product(s). Similar to Fc1, Fc2 displayed an irreversible indole oxidation wave at *ca.* +0.95 and a quasi-reversible couple at *ca.* +1.20 V. After this indole oxidation, a new ferrocenium/ferrocene couple was established at *ca.* +0.55 V (Fig. 4b). This anodic shift of the potential could be due to the adsorption of the oxidised products of Fc2 onto the electrode surface. Fc3 showed similar electrochemical properties; the indole oxidation occurred at +0.93 V (irreversible) and +1.40 V (quasi-reversible) and the additional ferrocenium/ferrocene couple appeared at +0.53 V. We noted that the faradaic currents of the ferrocenium/ferrocene redox couples of all three compounds increased linearly with the square root of the sweep rates, suggestive of a diffusion-controlled process. The diffusion coefficients of Fc1, Fc2 and Fc3 in CH_3CN were estimated to be *ca.* 6.4×10^{-6}, 6.1×10^{-6} and 5.2×10^{-6} cm^2 s^{-1}.[26]

Table 3 Selected bond distances (Å) and bond angles (°) for Fc2

C(1)–C(11)	1.495(3)	C(11)–N(1)	1.468(3)
C(12)–C(13)	1.517(3)	C(12)–N(1)	1.463(3)
C(13)–C(14)	1.506(3)	Fe(1)–C(1)	2.050(2)
Fe(1)–C(2)	2.040(2)	Fe(1)–C(3)	2.043(2)
Fe(1)–C(4)	2.047(2)	Fe(1)–C(5)	2.045(2)
Fe(1)–C(6)	2.039(2)	Fe(1)–C(7)	2.042(2)
Fe(1)–C(8)	2.042(2)	Fe(1)–C(9)	2.045(2)
Fe(1)–C(10)	2.053(2)		
C(1)–C(11)–N(1)	112.12(18)	C(2)–C(1)–C(11)	125.1(2)
C(5)–C(1)–C(11)	127.5(2)	C(11)–N(1)–C(12)	112.08(18)
C(12)–C(13)–C(14)	112.76(19)	C(13)–C(14)–C(15)	126.9(2)
C(13)–C(14)–C(21)	127.0(2)	C(13)–C(12)–N(1)	111.60(19)

Table 4 Electrochemical data of Fc1–Fc3 in CH_3CN (0.1 M TBAP) at 298 K (glassy carbon working electrode, sweep rate = 100 mV s^{-1}, all potentials *vs.* SCE)

Compound	E_{pa}/V	E_{pc}/V	$E_{1/2}$/V	ΔE/mV
Fc1	+0.52	+0.45	+0.49	70
	+1.07	+0.84	+0.96	230
	+1.29	+1.25	+1.27	40
Fc2	+0.39	+0.32	+0.36	70
	+0.95	[a]	[a]	[a]
	+1.25	+1.15	+1.20	100
Fc3	+0.40	+0.32	+0.36	80
	+0.93	[a]	[a]	[a]
	+1.44	+1.35	+1.40	90

[a] No cathodic wave was observed.

Electrochemical titrations

Serum albumins are well known to bind small organic molecules such as indole, tryptamine and their derivatives.[8,9,13,27,28] The possible binding of the conjugates Fc1, Fc2 and Fc3 to BSA has been examined. Unfortunately, the imine group of

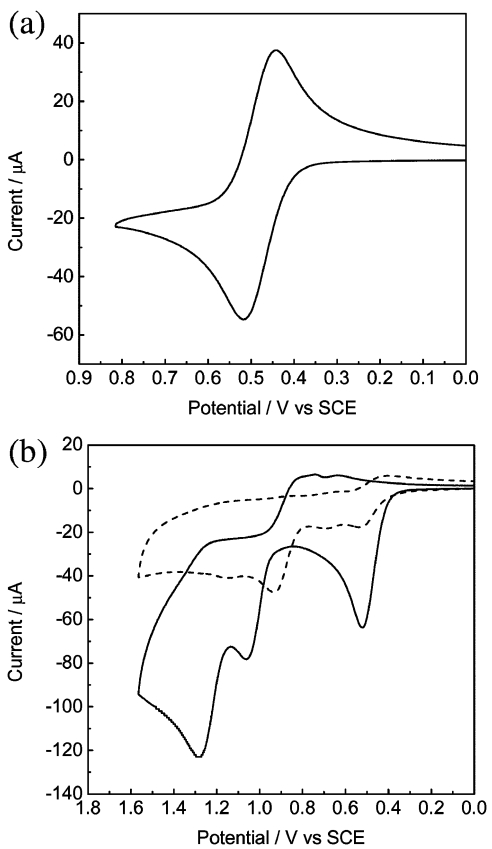

Fig. 3 Cyclic voltammograms of Fc1 in CH_3CN (0.1 M TBAP) at 298 K recorded in two potential windows (0.0 to +0.8 V and 0.0 to +1.6 V *vs.* SCE, respectively) using a glassy carbon working electrode at a sweep rate of 100 mV s^{-1} (first cycle (—), second cycle (--)).

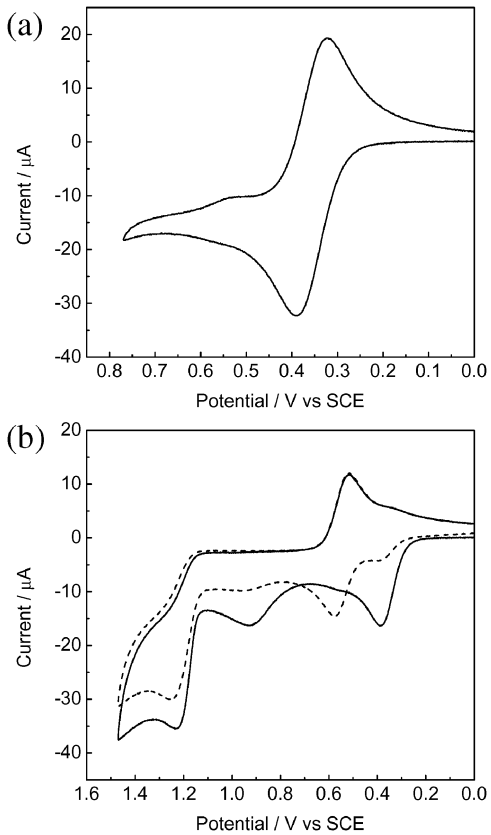

Fig. 4 Cyclic voltammograms of Fc2 in CH_3CN (0.1 M TBAP) at 298 K recorded in two potential windows (0.0 to +0.8 V and 0.0 to +1.6 V *vs.* SCE, respectively) using a glassy carbon working electrode at a sweep rate of 100 mV s^{-1} (first cycle (—), second cycle (--)).

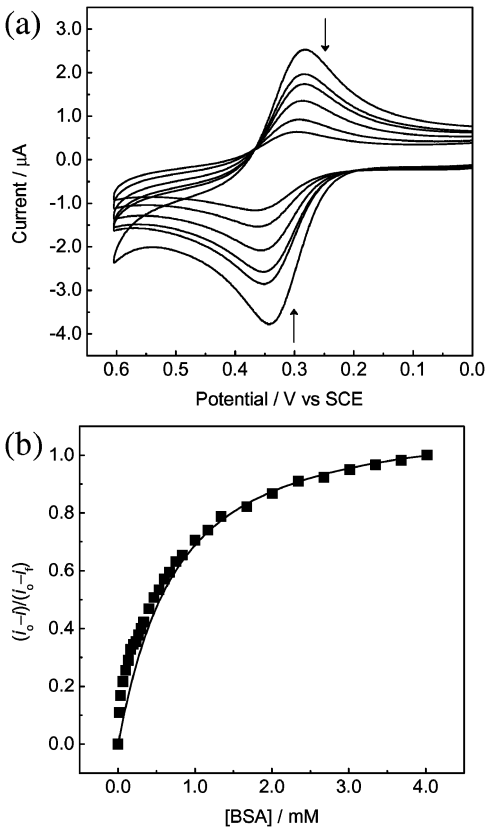

Fig. 5 (a) Cyclic voltammograms of Fc2 (0.28 mM) in phosphate buffer upon addition of BSA at 298 K. The concentrations of BSA were 0, 167, 335, 670, 1339 and 2678 μM, respectively. (b) A plot of $(i_o - i)/(i_o - i_f)$ *vs.* [BSA] for Fc2 (■) and its theoretical fit (—) using eqn (1) and (2).

Fc1 undergoes hydrolysis in aqueous solutions, limiting its use as a protein probe. Cyclic voltammograms of Fc2 and Fc3 in phosphate buffer upon addition of BSA are illustrated in Fig. 5a and 6a, respectively. The peak currents of the ferrocenium/ferrocene couples of both Fc2 and Fc3 were reduced by *ca.* 77% in the presence of BSA. The decrease is mainly due to binding of the indole moieties to the protein, leading to a reduction of the diffusion coefficients of the ferrocene compounds.[29] The binding constants (K_s) of Fc2 and Fc3 to BSA have been determined using eqn (1) and (2). Plots of $(i_o - i)/(i_o - i_f)$ *vs.* [BSA] and the theoretical fits for Fc2 and Fc3 are shown in Fig. 5b and 6b, respectively. The K_s values of Fc2 and Fc3 were determined to be *ca.* 3.8×10^3 ($s = 1.3$) and 4.7×10^3 M^{-1} ($s = 1.5$), respectively. These values are smaller than those of tryptamine (1.1×10^4 M^{-1}), indole-3-acetic acid (1.7×10^4 M^{-1}) and 5-hydroxyindole-3-acetic acid (2.0×10^4 M^{-1}),[8] most likely due to the relatively bulky ferrocene moiety. Nevertheless, the steric hindrance between the protein and ferrocene can be reduced using a spacer-arm, as evidenced by the observation that Fc3 showed stronger binding to BSA than Fc2.

Luminescence titrations

The protein-binding properties of Fc2 and Fc3 have been investigated by emission titrations using a luminescent BSA conjugate. Similar to other luminescent d^6 transition metal polypyridine systems, the emission of the complex $[Ir(ppy)_2(phen)](PF_6)$ is quenched by ferrocene.[30–32] Our strategy is to make use of the emission quenching of a luminescent BSA conjugate labelled with $[Ir(ppy)_2(phen\text{-}N{=}C{=}S)](PF_6)$,[16] Ir-BSA, by the ferrocene moieties of Fc2 and Fc3. We anticipate that if the indole moieties of Fc2 and Fc3 bind to BSA, the ferrocene pendants would be brought closer to the immoblilised iridium(III) complexes, resulting in more efficient emission quenching. The emission spectral traces for the titrations of Ir-BSA with Fc2 and Fc3 are illustrated in Fig. 7a and 8a, respectively. As expected, upon addition of the ferrocene probes, the emission intensity of Ir-BSA was substantially decreased by *ca.* 88% for Fc2 and *ca.* 96% for Fc3. Unmodified ferrocene also caused some emission quenching but the decrease was much smaller (<15%). Importantly, unmodified indole had no effects on the emission properties of the Ir-BSA conjugate. Thus, it is likely that the quenching caused by the current probes is a combined effect of the indole and ferrocene moieties of Fc2 and Fc3, and that the binding of the indole units of these compounds to BSA enhances the efficiency of quenching by ferrocene. The binding constants (K_s) of Fc2 and Fc3 to Ir-BSA were determined to be *ca.* 3.7×10^3 and 4.9×10^3 M^{-1}, respectively, using eqn (3) based on the assumption of a 1 : 1 binding model (Fig. 7b and 8b). The K_s

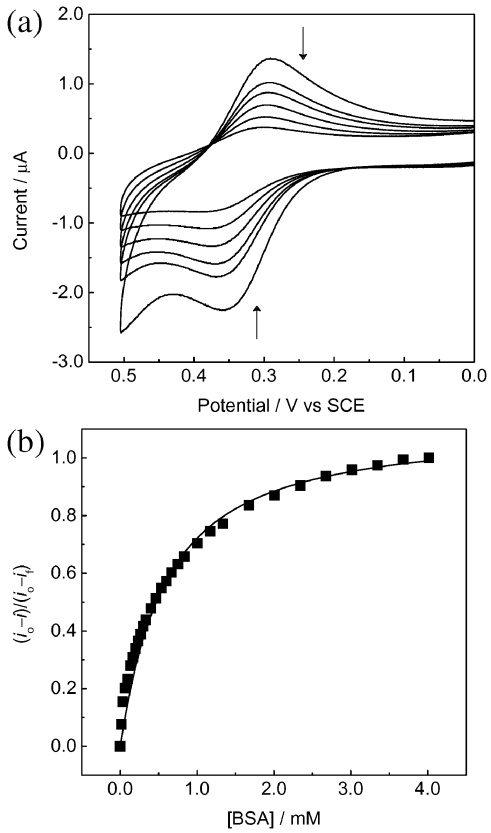

Fig. 6 (a) Cyclic voltammograms of Fc3 (0.28 mM) in phosphate buffer upon addition of BSA at 298 K. The concentrations of BSA were 0, 167, 335, 670, 1339 and 2678 μM, respectively. (b) A plot of $(i_o - i)/(i_o - i_f)$ *vs.* [BSA] for Fc3 (■) and its theoretical fit (—) using eqn (1) and (2).

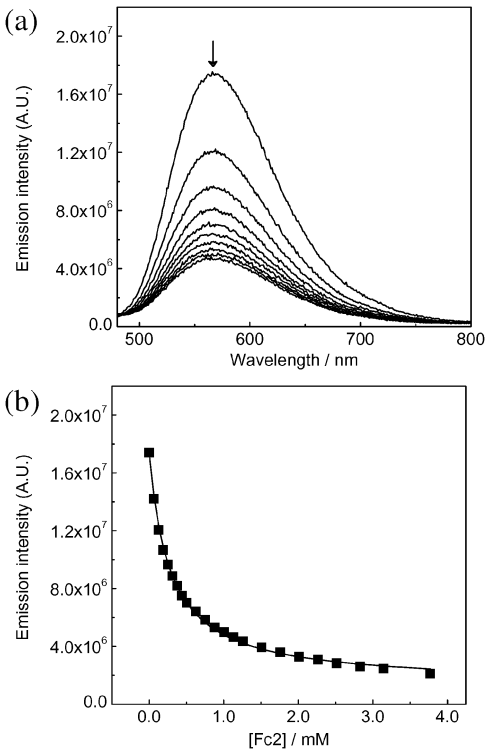

Fig. 7 (a) Emission spectral traces of Ir-BSA (7.58 μM) in phosphate buffer upon addition of Fc2 at 298 K. The concentrations of Fc2 were 0, 126, 251, 377, 503, 629, 754, 880, 1006 and 1131 μM, respectively. (b) A plot of emission intensity of Ir-BSA (7.58 μM) at 567 nm (■) *vs.* [Fc2] and its theoretical fit (—) using eqn (3).

value of Fc3 is larger than that of Fc2, which is in good agreement with the results obtained from the electrochemical titrations. The binding probably occurs at a hydrophobic substrate-binding site (site II) of BSA, which is well known to have a high affinity for aromatic compounds such as L-tryptophan.[28]

Tryptophanase inhibition assays

The enzyme TPase catalyses a variety of α,β-elimination and β-replacement reactions of amino acid substrates in the presence of the cofactor pyridoxal 5-phosphate; for example, it catalyses the conversion of L-serine to pyruvate. It has been shown that indole inhibits the activity of this enzyme.[12] The inhibition of enzymatic activity by small molecules is important as it is a major mechanism in controlling biological systems. In order to study the possible inhibition of TPase by the current ferrocene–indole compounds, a standard assay based on the conversion of L-serine to pyruvate by the enzyme has been performed.[12] The formation of pyruvate was coupled to the LDH/NADH system and the consumption of NADH was accompanied by the decrease of the absorbance of the reaction mixture at 340 nm. Plots of v^{-1} *vs.* [L-serine]$^{-1}$ for the TPase inhibition assays using Fc2, Fc3, ferrocene, indole and when no inhibitor was used are shown in Fig. 9. At [L-serine] = 800 mM, free indole inhibited *ca.* 57% of the enzyme activities, while Fc2 and Fc3 caused *ca.* 30 and 51% inhibition, respectively. Under our experimental conditions, ferrocene only showed <10% inhibition. It appears that the inhibition by Fc2 and Fc3 mainly originates from the binding of their indole moieties to TPase. The results also indicate that Fc3 inhibits the activity of TPase more effectively than Fc2, probably due to lower steric hindrance between the ferrocene moiety and the enzyme. From the *x*-intercepts of the linear fits, the K_m values were determined to be *ca.* 149, 157 and 150 mM for Fc2, Fc3 and indole, respectively. Since the *x*-intercepts for all the curves are similar, Fc2, Fc3 and indole inhibited the TPase-catalysed conversion of L-serine to pyruvate in a similar fashion, supporting the argument that the indole moiety of the ferrocene probes is responsible for the inhibition. The two ferrocene probes gave similar K_m values, indicating that although the spacer-arm of Fc3 can cause a higher degree of inhibition, it did not significantly affect the binding affinity of L-serine to the enzyme.

Conclusions

This paper describes the synthesis, characterisation and electrochemical properties of three redox-active ferrocene–indole compounds Fc1, Fc2 and Fc3. The X-ray crystal structures of Fc1 and Fc2 have been investigated. The protein-binding properties of Fc2 and Fc3 have been studied. The results

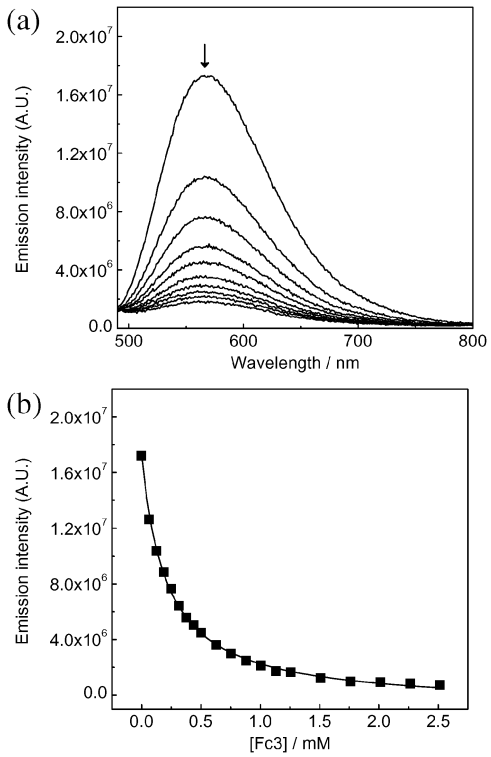

Fig. 8 (a) Emission spectral traces of Ir-BSA (7.58 μM) in phosphate buffer upon addition of Fc3 at 298 K. The concentrations of Fc3 were 0, 126, 251, 377, 503, 629, 754, 880, 1006 and 1131 μM, respectively. (b) A plot of emission intensity of Ir-BSA (7.58 μM) at 567 nm (■) *vs.* [Fc3] and its theoretical fit (—) using eqn (3).

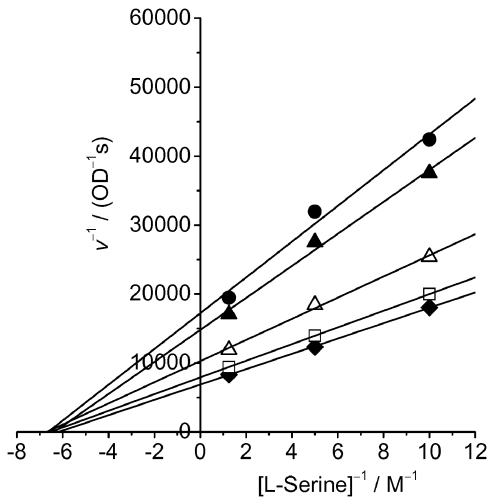

Fig. 9 Plots of v^{-1} *vs.* [L-serine]$^{-1}$ for TPase inhibition assays, in which inhibitors Fc2 (△), Fc3 (▲), Fc (□) and indole (●) were employed, or when no inhibitor (◆) was used.

revealed that Fc2 and Fc3 can be recognised by indole-binding proteins including BSA, iridium-modified BSA and TPase. The spacer-arm of Fc3 facilitates its binding to these proteins as a result of reduced steric hindrance between the ferrocene units and the biological hosts. We anticipate that related redox-active indole conjugates can be utilised as new probes for indole-binding proteins.

Acknowledgements

We thank the Hong Kong Research Grants Council (Project No. CityU 101704) for financial support. J.S.-Y.L. acknowledges the receipt of a Postgraduate Studentship and a Research Tuition Scholarship, both administered by City University of Hong Kong. We are also grateful to Faculty of Science and Engineering of City University of Hong Kong for support (Project No. 9610020).

References

1 B. Bartel, *Annu. Rev. Plant Physiol. Plant Mol. Biol.*, 1997, **48**, 51.
2 K. Ljung, A. K. Hull, M. Kowalczyk, A. Marchant, J. Celenza, J. D. Cohen and G. Sandberg, *Plant Mol. Biol.*, 2002, **50**, 309.
3 (*a*) P. M. Nair and C. S. Vaidyanathan, *Biochim. Biophys. Acta*, 1964, **81**, 496; (*b*) S. P. Kunaouli and C. S. Vaidyanathan, *Plant Physiol.*, 1983, **71**, 19.
4 C. S. Pundir, G. K. Garg and V. S. Rathore, *Phytochemistry*, 1984, **23**, 2423.
5 T. Niwa, M. Ise and T. Mitazaki, *Am. J. Nephrol.*, 1994, **14**, 207.
6 (*a*) F. Hirata and O. Hayaishi, *Biochem. Biophys. Res. Commun.*, 1972, **47**, 1112; (*b*) F. Hirata, O. Hayaishi, T. Tokuyama and S. Senoh, *J. Biol. Chem.*, 1974, **249**, 1311.
7 N. E. Schore and N. J. Turro, *J. Am. Chem. Soc.*, 1975, **97**, 2488.
8 N. Okabe and K. Adachi, *Chem. Pharm. Bull.*, 1992, **40**, 499.
9 A. Mazzini, P. Cavatorta, M. Iori, R. Favilla and G. Sartor, *Biophys. Chem.*, 1992, **42**, 101.
10 J. Bilang, H. Macdonald, P. J. King and A. Sturm, *Plant Physiol.*, 1993, **102**, 29.
11 R. Zettl, J. Schell and K. Palme, *Proc. Natl. Acad. Sci. USA*, 1994, **91**, 689.
12 I. D. A. Swan, *J. Mol. Biol.*, 1972, **65**, 59.
13 E. Doluić, M. Kowalczyk, V. Magnus, G. Sandberg and J. Normanly, *Bioconjugate Chem.*, 2001, **12**, 152.
14 (*a*) K. K.-W. Lo, K. H.-K. Tsang, W.-K. Hui and N. Zhu, *Chem. Commun.*, 2003, 2704; (*b*) K. K.-W. Lo, K. H.-K. Tsang, W.-K. Hui and N. Zhu, *Inorg. Chem.*, 2005, **44**, 6100; (*c*) K. K.-W. Lo, T. K.-M. Lee and Y. Zhang, *Inorg. Chim. Acta*, 2006, **359**, 1845.
15 D. D. Perrin and W. L. F. Armarego, *Purification of Laboratory Chemicals*, Pergamon, Oxford, 1997.
16 K. K.-W. Lo, C.-K. Chung, T. K.-M. Lee, L.-H. Lui, K. H.-K. Tsang and N. Zhu, *Inorg. Chem.*, 2003, **42**, 6886.
17 Z. Otwinowski and W. Minor, *Methods Enzymol.*, 1997, **276**, 307.
18 A. Altomare, M. C. Burla, M. Camalli, G. L. Cascarano, C. Giacovazzo, A. Guagliardi, A. G. G. Moliterni, G. Polidari and R. Spagna, *J. Appl. Crystallogr.*, 1999, **32**, 115.
19 G. M. Sheldrick, *Programs for Crystal Structure Analysis (Release 97–2)*, University of Göttingen, Germany, 1997.
20 M. T. Carter, M. Rodriguez and A. J. Bard, *J. Am. Chem. Soc.*, 1989, **111**, 8901.
21 M. M. Bradford, *Anal. Biochem.*, 1976, **72**, 248.
22 J. Bourson, J. Pouget and B. Valeur, *J. Phys. Chem.*, 1993, **97**, 4552.
23 G. L. Atkins and I. A. Nimmo, *Biochem. J.*, 1973, **135**, 779.
24 H.-B. Kraatz, *J. Organomet. Chem.*, 1999, **579**, 222.
25 K. K.-W. Lo, J. S.-Y. Lau, D. C.-M. Ng and N. Zhu, *J. Chem. Soc., Dalton Trans.*, 2002, 1753.
26 A. J. Bard and L. R. Faulkner, *Electrochemical Methods, Fundamentals and Applications*, Wiley, New York, USA, 2nd edn, 2001, p. 218.
27 F. A. De Wolf and G. M. Brett, *Phamacol. Rev.*, 2000, **52**, 207.
28 L. Fielding, S. Rutherford and D. Fletcher, *Magn. Reson. Chem.*, 2005, **43**, 463.
29 Addition of ferrocene also induced a decrease of the faradaic current. However, the extent of the decrease was very small compared to the cases of Fc2 and Fc3. Also, no satisfactory fits were obtained by fitting the data to eqn (1).

30 U. Siemeling, J. Vor der Brüggen, U. Vorfeld, B. Neumann, A. Stammler, H.-G. Stammler, A. Brockhinke, R. Plessow, P. Zanello, F. Laschi, F. Fabrizi de Biani, M. Fontani, S. Steenken, M. Stapper and G. Gurzadyan, *Chem. Eur. J.*, 2003, **9**, 2819.
31 A. Delgadillo, A. M. Leiva and B. Loeb, *Polyhedron*, 2005, **24**, 1749.
32 E. J. Lee and M. S. Wrighton, *J. Am. Chem. Soc.*, 1991, **113**, 8562.